AWARD NUMBER: W81XWH-17-1-0525

TITLE: Iron Chelation Enhances TAM and Triple-Negative Breast Cancer Cell Death

PRINCIPAL INVESTIGATOR: Jason Koutcher

CONTRACTING ORGANIZATION: Sloan Kettering Institute for Cancer Research
New York, NY 10065

REPORT DATE: OCTOBER 2019

TYPE OF REPORT: Annual Technical

PREPARED FOR: U.S. Army Medical Research and Materiel Command
Fort Detrick, Maryland 21702-5012

REPORT DOCUMENTATION PAGE

Form Approved
OMB No. 0704-0188

1. REPORT DATE	2. REPORT TYPE	3. DATES COVERED
OCTOBER 2019	Annual	15 Sept 2018 – 14 Sept 2019

4. TITLE AND SUBTITLE
Iron Chelation Enhances TAM and Triple-Negative Breast Cancer Cell Death

5a. CONTRACT NUMBER

5b. GRANT NUMBER W81XWH-17-1-0525

5c. PROGRAM ELEMENT NUMBER

6. AUTHOR(S)
Jason Koutcher (initiating PI) and Ronald Blasberg (Partnering PI)

E-Mail: koutchej@mskcc.org ; blasberr@mskcc.org

5d. PROJECT NUMBER

5e. TASK NUMBER

5f. WORK UNIT NUMBER

7. PERFORMING ORGANIZATION NAME(S) AND ADDRESS(ES)
Sloan Kettering Institute for Cancer Research
1275 York Avenue, New York, NY 10065-6007

8. PERFORMING ORGANIZATION REPORT NUMBER

9. SPONSORING / MONITORING AGENCY NAME(S) AND ADDRESS(ES)
U.S. Army Medical Research and Materiel Command
Fort Detrick, Maryland 21702-5012

10. SPONSOR/MONITOR'S ACRONYM(S)

11. SPONSOR/MONITOR'S REPORT NUMBER(S)

12. DISTRIBUTION / AVAILABILITY STATEMENT
Approved for Public Release; Distribution Unlimited

13. SUPPLEMENTARY NOTES

14. ABSTRACT The goal of this study is to complete preclinical testing of Deferiprone (DFP), an iron chelator in clinical use for non-oncologic diseases. To date we have demonstrated that DFP has an IC50 for TNBC within the range achieved after a clinical dose, and enhances the effect of taxol in 4T1 tumors. The IC50 for tumor cells was lower than measured for macrophages (M0, M1, M2)indicating potential therapeutic gain and safety in treating cancer cells. In 4T1 tumors, DFP did not change iron concentration measured in tissues (spleen and tumor). In perfused 4T1 cells, we demonstrated metabolic inhibition of the tricarboxylic acid cycle and lipid metabolism by DFP and similar studies are ongoing in the MDA-231. WE have measured lactate in tumors (control and DFP treated) and the data are currently undergoing analysis.

15. SUBJECT TERMS

15. SUBJECT TERMS
Breast cancer, iron imaging, MRI, metabolism

16. SECURITY CLASSIFICATION OF:			17. LIMITATION OF ABSTRACT	18. NUMBER OF PAGES	19a. NAME OF RESPONSIBLE PERSON
a. REPORT	b. ABSTRACT	c. THIS PAGE			USAMRMC
Unclassified	Unclassified	Unclassified	Unclassified	15	19b. TELEPHONE NUMBER *(include area code)*

Table of Contents

Page

Introduction
The goal of this study is to complete preclinical testing of Deferiprone (DFP), an iron chelator in clinical use for nononcologic diseases. We propose to demonstrate the sensitivity of TNBC to DFP as a single agent, and in combination with immune modulation therapy (checkpoint inhibitors) and chemotherapy (paclitaxel). We will determine if imaging of changes in iron content using magnetic resonance imaging can serve as a biomarker of DFP efficacy. Studies were planned to be performed sequentially by first studying in vitro effects of DFP, followed by in vivo effects, followed by the effects of adding other drugs (checkpoint inhibitors and paclitaxel). Effects of these drugs on cell
cycle and immune effects were also proposed

Keywords:
Breast cancer, MRI, iron, chelators, Deferiprone, macrophages, metabolism, checkpoint inhibitors

Major Goals of Projects:
Aim 1 Determine how inhibition of iron metabolism and OXPHOS impedes TAM function and metabolism, and reduces proliferation of TAMs and TNBC cells.
Aim 2: *Develop and validate non-invasive MRI methods to quantitatively and spatially monitor tumor and tissue iron and TAM infiltration, to detect changes induced by macrophage focused therapy*.
Aim 3: *Determine if inhibition of iron metabolism, TCA cycle, and OXPHOS by DFP: i) inhibits tumor growth, and ii) enhances responses to chemotherapy and immune checkpoint inhibitors in orthotopic TNBC*

Accomplishments (Summary):
1. Methodology for iron imaging in breast cancer has been developed and reported (see Year 1 report). This methodology was applied to the 4T1 breast cancer model as proposed (see Year 1 report) and we have acquired the data for the MDA-231 and present it.
2. In last year's report we noted a series of setbacks on the perfused cell apparatus (largely in the new NMR spectrometer) and only presented very preliminary data. In the current report, we have completely finished acquiring and analyzing the 4T1 data which we present (including a recent abstract), almost ½ of the data for the MDA-231 has also been acquired and the work is going relatively smoothly.
3. We have shown that macrophages are less sensitive to DFP than tumor cells which was a concern since some macrophages are essential for anti-tumor effects. We initially demonstrated that we could polarize M0 mouse macrophages into M1 and M2 macrophages. We subsequently measured IC50 of DFP in the M0, M1, and M2 macrophages and found that they were greater than the IC50 of tumor cells. These data indicate a therapeutic window for DFP at the proposed clinical dose wherein tumor cells are more sensitive than M0, M1, and M2 macrophages

What was Accomplished

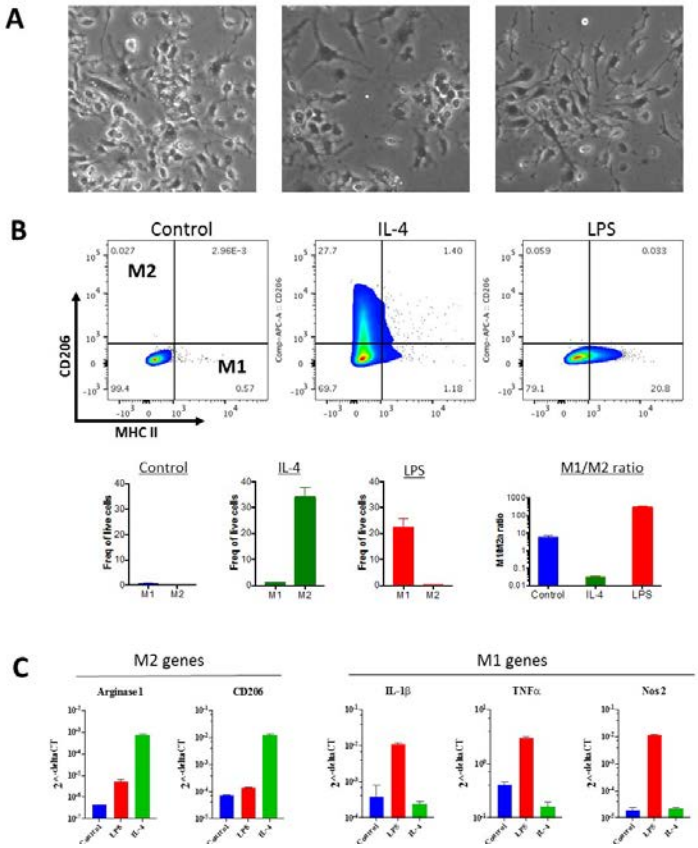

Fig. 1 RAW 264.7 cells were plated in 12 well plates (100,000 cells/well) with either 20ng/ml mouse IL4 or 100ng/ml LPS for up to 48 hours. A. Brightfield images of cells at 24 hours post stimulation. B, C: After 24 hours the cells were detached and processed for flow cytometry (B) and quantitative PCR (C)

A. Flow cytometry (Blasberg Laboratory) (Aim 1).

We cultured RAW 264.7 mouse macrophage cell line in the presence of either interleukin-4 (IL-4) or lipopolysaccharide (LPS) to polarize them towards an anti-inflammatory (M2 macrophages) or pro-inflammatory (M1 macrophage) phenotype, respectively. RAW 264.7 cells were plated in 12 well plates (100,000 cells/well) with either 20ng/ml mouse IL-4 or 100ng/ml LPS for up to 48 hours. After 24 hours, the cells cultured with IL-4 and LPS began to change their morphology into larger and more polarized cells (**Fig. 1A**). We detached these cells from the plates and examined surface expression of 2 markers of M1 and M2 macrophages (MHC class II and CD206) by flow cytometry (**Fig 1B**). RAW 264.7 cells at baseline do not express these markers (**Fig 1B**). Culturing these cells in IL-4 for 24 hours increased the expression of the M2 marker CD206 but had little to no effect on the M1 marker MHC II. This led to a decrease in the ratio of M1 to M2 macrophages tipping the balance towards anti-inflammatory macrophages. In contrast, culturing the cells in LPS increase expression of the M1 marker MHC II but had no effect on the expression of CD206. This led to an increase in the M1 to M2 ratio tipping the balance towards a pro-inflammatory phenotype. We confirmed the polarization of RAW 264.7 cells towards M2 and M1 macrophages after being cultured for 24 hours in the presence of IL-4 and LPS using quantitative PCR to examine gene expression of known M2 (CD206, Arg1) and M1 (IL-1b, TNFa, Nos2) genes (**Fig 1C**). In agreement with the flow cytometry data, IL-4 induced expression of M2 genes while LPS induced expression of M1 genes. Taken together these data support the conclusion that IL-4 re-programs RAW 264.7 cells towards an M2 macrophage phenotype while LPS re-programs these cells towards M1 macrophage phenotype.

B. Macrophage Sensitivity to DFP (Blasberg Laboratory) (Aim 1)

In Year 1, we had focused/performed cell studies to determine the sensitivity to various breast (and prostate) tumor cells to DFP and its effect on enhancing the effects of chemotherapy drugs. That data were presented in last year's report. We were pleased with the fact that IC50 (40-60 uM) and IC90 values were typically less than the serum values found after administration of DFP to volunteers (>100uM). However, efficacy is a balance of killing the cancer cells while minimizing damage to normal cells so in Year 2 we performed the proposed studies of macrophage sensitivity to DFP.

Measurements of macrophages IC50's were performed as previously described (1). The methodology differed only in that we studied RAW264.7 unpolarized macrophages and additionally studied M1 (exposed to lipopolysaccharide during incubation with DFP) and M2 (exposed to IL4 during incubation with DFP) polarized macrophages. Figure 1 above shows that we could successfully polarize M0 mouse macrophages into M1 and M2 macrophages. Cells (7×10^4) were plated and doses of 0, 16, 30, 66, 100, 160, 300, and 660 µM were studied. Time exposures ranged from 48-72 hours (M0) and 48 hours (M1, M2). A typical IC50 series of

curves are shown in Fig. 2 for M1 macrophages (48 hour exposure). Table 1 and Figure 3 summarize the results of these studies demonstrating that the IC50 values for polarized and unpolarized macrophages were higher (they are less sensitive to DFP) than breast cancer cells as we had hypothesized.

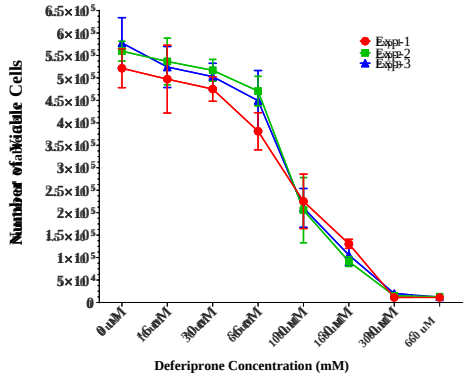

Fig. 2. M1 polarized cells exposed to DFP at different doses demonstrating similar sensitivity on all 3 studies

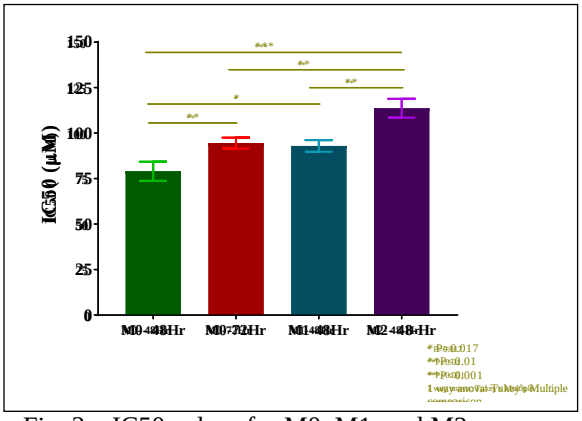

Fig. 3. IC50 values for M0, M1, and M2 macrophages and their differing sensitivities to DFP

Run	M0-48 hr	M0- 72 hr	M1-48 hr	M2-48 hr
1	80.78 μM	91.34 μM	96.62 μM	116.3 μM
2	73.13 μM	95.03 μM	90.77 μM	117 μM
3	83.21μM	97.21 μM	91.45μM	107.7 μM
Average	**79.04 ± 5.3 μM**	**94.53 ± 3μM**	**92.95 ± 3.2 μM**	**113.67 ± 5.2 μM**

Table 1. IC50 values for M0, M1, and M2 macrophages. In comparison to the tumor cell results presented in last year/s report, the macrophages are more resistant to DFP than tumor cells

C. Perfused cells (Koutcher Laboratory) (Aim 1)

In last year's report we showed preliminary spectra from perfused 4T1 breast cancer cells. At this point, we have completed the 4T1 studies (both 31P and 13C) and analyzed the data in terms of changes of metabolite ratios induced by exposure to DFP. The data were presented at the recent Molecular Imaging Society meeting (2). Appendix A is the poster presented and details how the perfused cells appear when growing on microcarrier beads, the setup in the magnet to ensure viability (bioreactor), the growth rate during the experiment (demonstrated that as in cell culture, DFP slows growth of tumor cells), and 31P and 13C MR spectra, and time course effect of DFP on metabolism.

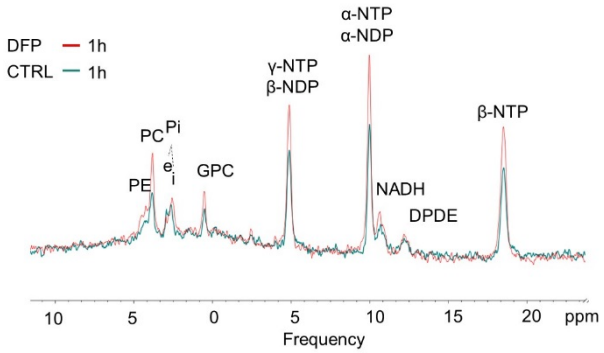

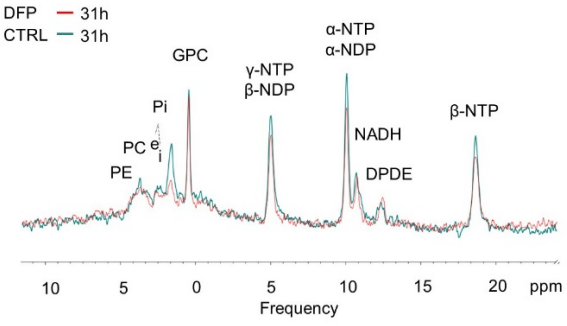

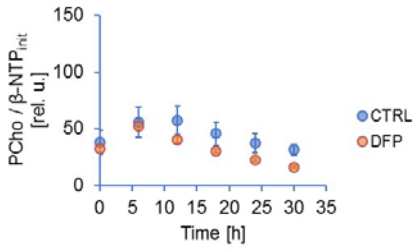

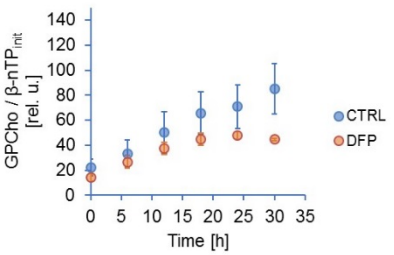

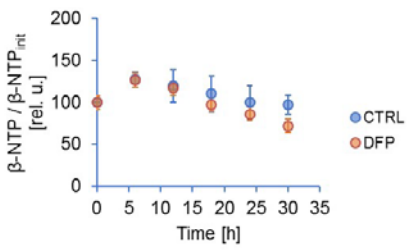

Fig. 4 Top left. 31P NMR spectra obtained in the first hour of cell perfusion with and without DFP as labelled (baseline). Top Right. 31P NMR spectra obtained after 31 hours of cell perfusion with and without DFP. Peak areas ratios were normalized to β-NTP which has been shown to be a measure of cell number.
Bottom: Changes in glycerophosphocholine, phosphocholine, and βNTP over time. Changes were significant after 18 hours . PE = phosphoethanolamine, PC=phosphocholine, Pi = inorganic phosphate (2 peaks - intra and extracellular), GPC = glycerophosphocholine, NDP= nucleoside diphosphate, NTP = nucleoside triphosphate, DPDE = diphosphodiesters, NADH = Nicotine adenine dinucleotide (reduced and oxidized)

The 31P MR spectra are shown in Fig. 4. We compared DFP-treated and control cells, acquired at the start (left) and end (right) of the experiment. Time course curves for phosphocholine (Pcho), glycerophosphocholine (GPCho), and β-NTP (nucleoside triphosphate) showed statistically significant changes ($p < 0.05$, unpaired t-test) between DFP-treated and control cells (Bottom). Three independent experiments were done for untreated and DFP treated cells.

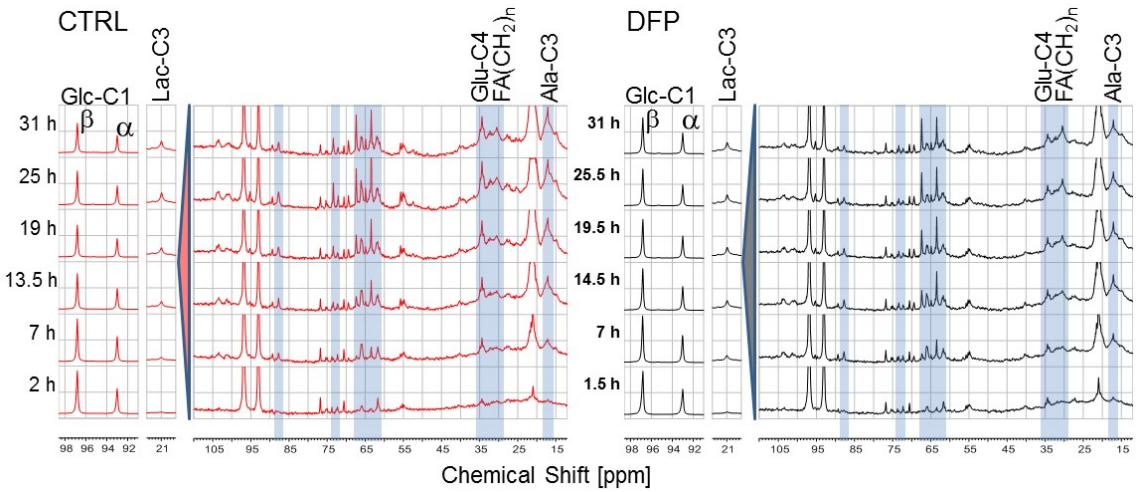

Fig. 5. Serial 13C NMR spectra of 4T1 cells perfused with 1-13C glucose as a label and media or 100 uM DFP. Not all peaks are labelled because of their density but over 200 peaks were assigned and analyzed. We have performed these measurements on 3 independent studies of control and DFP treated 4T1 cells and are in the process of performing similar studies on the MDA-231 cells

To analyze biochemical changes that occurred in response to DFP in greater depth, we perfused the cells with 1-13C-glucose and monitored changes in metabolism (Fig. 5). Quantitative evaluation of ^{13}C NMR spectral metabolites of DFP-treated cells revealed lower residual glucose (higher glucose consumption), decreased glutamine-$^{13}C4$ (decreased tricarboxylic acid cycle activity), and fatty acid chain synthesis, decreased glycerol-3-phosphate, and less alanine-C3 ^{13}C-labelling, among other changes, compared to control (CTRL) cells (Fig. 6). We are comparing these findings with our previous results in prostate cancer (1) and are in the process of accumulating equivalent data for the MDA-231. The acquisition of the latter data is almost ½ way done and will be presented in next year's report.

D. Cell Migration Studies (Koutcher and Blasberg Laboratory) (Aim 1)

We analyzed the effects of DFP on cell migration as a model for the initiation of the metastatic process, using a wound healing assay. Methods: For the wound healing assay, $3.1x10^4$ 4T1 cells / 0.4 ml culture medium were seeded in 24-well plates to attach and grow confluent. At 48 h post seeding, a "plus" sign was scratched across each well (**Fig. 7A**), using a 200 µl pipette attached to an aspirator, aspirating the medium and cell debris. Post scratch, each well was washed once with 1x PBS, followed by the addition of culture medium, containing either 0 µM, 50 µM, or 100 µM DFP, with 6 wells assigned to each condition. One image file/plate was acquired ~ every 12 h, starting at ~1 h after exposing cells to varying doses of DFP (t0), with brightfield microscopy (ZEN microscope, Carl Zeiss, Germany) using a 5x objective lens and 45 frames/well. During imaging, the plate was kept at 37 ˚C and 5% CO_2 in air in a microscope chamber for plates. To avoid nutrient depletion and medium

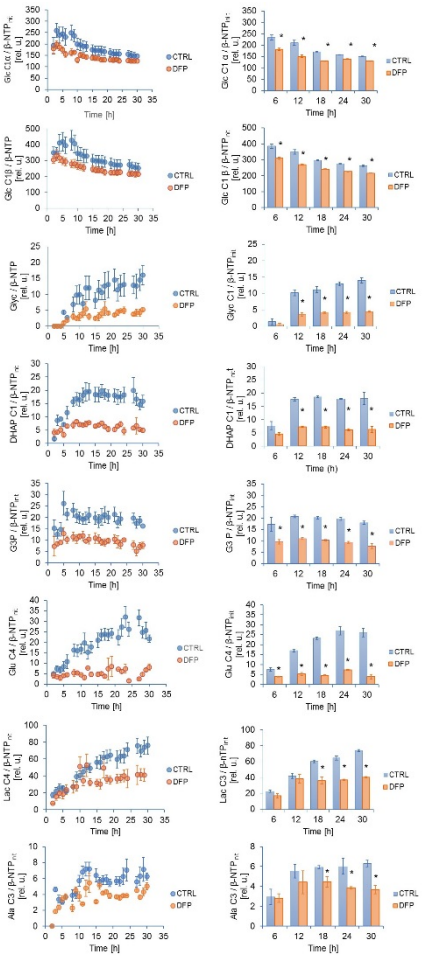

Fig. 6. Changes in metabolites over time for 4T1 cells untreated or treated with DFP (100uM). DFP induces changes in lipid and TCA metabolism based on changes noted in glycerol-3-P04 and ^{13}C4-glutamate.

acidification, culture media were changed every 24 h post seeding. An initial, separate 24 h wound healing experiment was performed to assess the time line of wound closure (data not shown), resulting in the choice of 48 h total imaging time with a 12 h time resolution.

Using the ZEN software, frames were stitched to form a single image covering the well and exported as Tiff images (1 image / well and time point) for further processing (**Fig. 7A**). A custom-written macro (Fiji) was used to automate the processing of the images to determine the open wound area at each time point and each well (**Fig. 7**). Images were converted to 8-bit images, background subtracted, unsharp and despeckling applied, followed by a variance filter and Gaussian blur filter to identify areas devoid of cells, as well as areas of lower cell density, surrounding the scratch (**Fig. 7B**). Only the central, circular region with sufficient contrast was quantified (**Fig. 7B**). Three independent experiments were acquired with 4T1 cells from different freeze dates or passage numbers. For each experiment, the images and analysis were reviewed for each well and wells with cell detachment or air bubbles affecting analysis were excluded from further quantification; per experiment and DFP dose, a maximum of 1 well was excluded, leaving 5 or 6 wells for averaging. For each DFP dose, a relative open wound area was calculated by dividing the absolute open wound area in µm^2 for each well and acquisition time point by the average of the absolute open wound area in µm^2 of all wells (n = 5 or 6) at t0. Thus, inter- and intra-experimental variations in wound area at the start of the experiments can be assessed and accounted for. For each of the 3 independent experiments, the mean ± SD of the relative open wound area were calculated for each condition. The mean average relative open wound area at each time point and for each condition was then averaged for the three independent experiments and the corresponding SD calculated by error propagation (maximum error, assuming Gaussian distribution). For later time points when all wells per experiment and condition had a fully closed wound area (relative open wound area = 0 %), as seen for the untreated cells, the measurement error was defined to be zero.

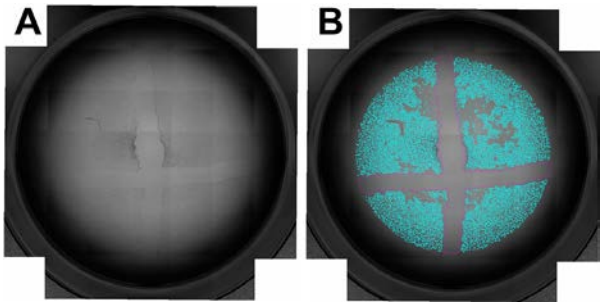

Figure 7: (A) Representative image of a well with confluent 4T1 cells at the first imaging time point, depicting the 2 scratch lines across the well at the start of the experiment. 2.58 µm x 2.58 µm x 1 µm pixel size (~6680 x 6680 pixels in-plane, numbers approximate due to stitching of the frames, leading to up-to ~5% variation in total analyzed area) **(B)** Image in (A) overlaid with region selections: Magenta outline – open wound area (µm^2); Cyan outline – areas with less cell density, depicting cell density variations across 'homogenously' confluent 4T1 cells.

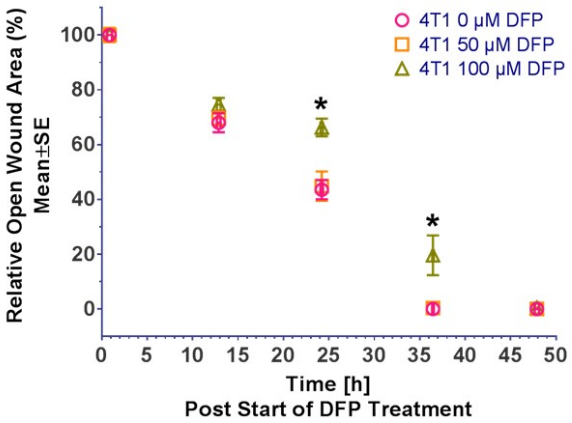

Figure 8: Wound closure as function of DFP exposure time for cells treated with 0 µM, 50 µM, and 100 µM DFP, respectively. Average of 3 independent experiments, with number of wells / experiment and DFP dose of n=5, 5, 5 for 0 µM DFP, n = 5, 6, 6 for 50 µM, and n = 6, 6, 6 for 100 µM DFP respectively

Results: Overall relative wound closure over time in

response to DFP exposure is displayed for 4T1 as mean ± SE (n = 3) in **Fig. 8**. Statistical differences between treatment groups were assessed by 2-way ANOVA with Tukey multiple comparison (swapped direction of comparisons). As shown in **Fig. 8**, untreated 4T1 cells closed the scratches completely by 36 h, undistinguishable from 4T1 cells treated with 50 µM DFP (~IC_{50} for 4T1 cells). Exposure of 4T1 cells to 100 µM DFP (~IC_{90} for 4T1 cells) delays full wound closure (i.e. inhibits cell migration required in the metastatic process) to 48 h, resulting in a significantly higher relative open wound area at 24 h (*P<0.0001*) and 36 h (*P=0.0003*) compared to untreated 4T1 cells and 4T1 cells treated with 50 µM DFP (**Fig. 8**). Parallel experiments are being completed on the MDA-231 breast cancer cell line.

E. Iron studies; Koutcher Laboratory (Aim 2) - MRI measurements of tissue iron in the MDA-MB-231.

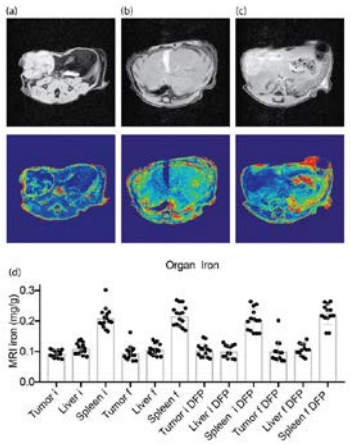

Figure 9. Iron MRI of MDA-MB-231 model in DFP trial. (upper) Gradient echo MRI and (lower) iron MRI maps for representative (a) tumor, (b) liver, and (c) spleen of Athymic nude mouse in MDA-MB-231 trial (7T body coil, TR/TE 2s/3ms, 0.1mm × 0.1mm × 1mm, 4 averages). (d) Mean organ iron values measured from iron MRI maps in control and deferiprone (DFP) treated mice bearing tumors with at initial (i) 150mm^3, and final (f) 500mm^3 timepoints. Points are measurements from individual mice (n=14-16 control, n=13-14 DFP). No significant differences are observed according to matched one-way ANOVA mixed effects model with multiple comparisons between iron values of like organs in the treatment groups and timepoints evaluated according to Tukey correction with P<0.05 cutoff. Statistics comparing different organs are not shown (e.g. tumor vs. spleen).

In last year's report, we presented the data for the 4T1 tumor bearing mice. We repeat the methodology for the sake of completeness for the MDA-MB-231 human breast cancer cell model. Methods: Gradient echo T_2^* MRI relaxometry was performed to characterize iron in spleen, liver, and mammary tumor in the Athymic nude MDA-MB-231 model. Deferiprone was administered at 150mg/kg daily starting at a tumor volume of approximately 150mm^3 (i=initial), and 500mm^3 (f=final). The MRI measurements were conducted at 7T using a body coil (TR/TE 2s/3ms, 0.1mm × 0.1mm × 1mm, 4 averages). Iron level was quantified according to iron calibration curve and mean iron level was measured within region-of-interests drawn over liver, spleen, or mammary tumor. To characterize the spatial distribution of macrophage iron deposits in the mammary tumors the iron map was stratified in the high-iron range and the pixel cluster analysis tool of ImageJ was used to quantify the total number of high-iron pixel clusters as a function of tumor position (% infiltration).

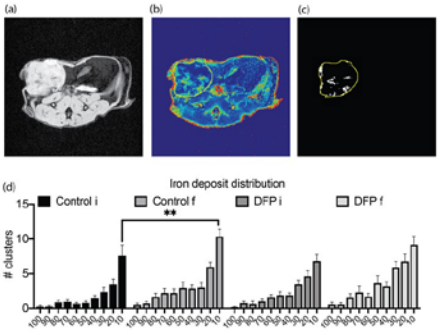

Figure 10. High-iron cluster spatial distributions of MDA-MB-231 DFP trial. (a) Representative gradient echo MRI showing breast tumor of Athymic nude mouse tumor in MDA-MB-231 trial at 500mm^3 (b) Iron map from multi-gradient echo T_2^* MRI showing breast tumor and ROI area (c) Stratified iron map (0.15-0.3 mg g^{-1}) from iron map in (b). showing high-iron pixel clusters. (d) Spatial distribution of number (#) of clusters as a function of % infiltration in the tumor in control and deferiprone (DFP) treated mice bearing tumors with average sizes of 150mm^3 (i=initial), and 500mm^3 (f=final). (mean +/- s.e.m. ** p=0.0023, unpaired t-test with Holm-Sidak multiple comparison correction).

Figure 9 and 10 summarize the results from MRI analysis of iron in spleen, liver and mammary tumor. Figure 9 demonstrates that overall tissue iron levels did not vary significantly either between measurements made at the various tumor burdens (i=initial, 150mm^3; f=final, 500mm^3), or deferiprone (DFP) treatment at these timepoints according to matched one-way ANOVA mixed effects model with multiple comparisons between iron values according to Tukey correction with P<0.05 cutoff. Image analysis of mammary tumors for high-iron pixels in Figure 10 revealed indications of iron deposits across the various cohorts. Most tumors appeared to contain high-iron pixel clusters within the tumor cross-sections that decreased with increasing distance from the outer tumor margin. A small increase was detected in number of these high-iron clusters between (i) 150mm^3 and (f) 500mm^3 measurement groups in both the control and DFP treated cohorts at the outermost decile regions of the infiltration profile, and statistical analysis of these distributions only reached significance for the control group between the initial (i)

and final (f) timepoints in the 10% region of the profile (p=0.0023, unpaired t-test with Holm-Sidak multiple comparison correction).

F. Effect of DFP on In Vivo Lactate metabolism (Aim 3Ai) (Koutcher Laboratory)

The data for both DFP and control tumors has been acquired for the 4T1 and are currently being analyzed. The acquisition of the data for the MDA-231 are almost completed. This will be presented in next year's report

G. Effects of DFP on oxidative phosphorylation and glycolysis as measured by XF-96 analyzer (Blasberg Laboratory) (Aim 1)

These studies were delayed by the departure of Ms. Kruchevsky who had been trained to do these studies. They are expected to be done in Year 3 when Mr. Winkleman becomes proficient in them. We focused on the cell migration (see above) instead

References

1. Simões RC, Veeraperumal S, Serganova IS, Kruchevsky N, Varshavsky J, Blasberg RG, Ackerstaff E, and Koutcher JA. Inhibition of prostate cancer growth by Deferiprone. NMR in Biomedicine, 2017 Jun;30(6). doi: 10.1002/nbm.3712. Epub 2017 Mar 8

2. Porcari P, LeKaye HC, Koutcher JA, Ackerstaff E. Iron Chelation Affects Cell Growth and Metabolism in the Triple-negative Breast Cancer Cell Line 4T1. Proceedings of the World Molecular Imaging Congress, 2019, September 4-7, Montreal, Canada.

Opportunities for Training and Development:
As noted in last year's report, Dr. Porcari has been supported and performing much of the work presented. She was first author on an abstract based on the work performed on this grant, and as noted below, we plan to write a manuscript shortly. Dr. Leftin, a postdoctoral fellow who had done all the iron studies, successfully applied for a faculty position at State University of NY (SUNY), Stony Brook and is an Assistant Professor of Chemistry and Radiology. He is continuing this work theme independently, although he and Dr. Koutcher have applied for a grant together with Dr. Leftin being the Corresponding PI.

How were the results disseminated?
In year 1, we noted two publications. This year we had an abstract presented (Reference 2) and hope to write a manuscript on this (and other parts of the application) material in Year 3

Next Reporting Period Goals:
1. Complete perfused cell metabolic studies on MDA-231 (almost ½ of data is acquired)
2. Analyze in vivo lactate data (almost all data acquired; analysis recently started)
3. In vivo studies in Aim 3
    a. 3Ai - *Effect of **DFP** (as a **single agent**)*: - data being analyzed
    b. 3Aii *Effect of **DFP** (in **combination with chemotherapy drugs (paclitaxel and cisplatin**);*
    c. 3Aiii *Effect of **DFP** (in **combination with immune checkpoint inhibitors***
4. Obtain no cost extension – It is likely more time will be needed for the extensive data analysis required (in vivo lactate data) and to complete Aim 3.

Impact:
Nothing to report.

Changes and Problems:
1. Our preliminary analysis suggests only modest in vivo effects of DFP on 4T1. This is not totally surprising since triple negative breast cancer tumors are highly resistant. We are optimistic that adding other therapies as proposed will yield benefit. If time allows we may seek authorization for studying an additional model

Products:

1. Porcari P, LeKaye HC, Koutcher JA, Ackerstaff E. Iron Chelation Affects Cell Growth and Metabolism in the Triple-negative Breast Cancer Cell Line 4T1. Proceedings of the World Molecular Imaging Congress, 2019, September 4-7, Montreal, Canada. (Reference 2)
2. Leftin A, Ben-Chetrit N, Joyce JA, Koutcher JA Imaging endogenous macrophage iron deposits reveals a metabolic biomarker of polarized tumor macrophage infiltration and response to CSF1R breast cancer immunotherapy. Nature Scientific Reports; 2019 Jan 29;9(1):857. (reported last year as "In Press")
3. Leftin A and Koutcher JA. Quantification of Nanoparticle Enhancement in Polarized Breast Tumor Macrophage Deposits by Spatial Analysis of MRI and Histological Iron Contrast Using Computer Vision. Contrast Media & Molecular Imaging. 2018 Oct 30;2018 (Reported last year as "In Press")

Participants:

Koutcher Laboratory; W81XWH-17-1-0525 (Initiating PI)

Jason Koutcher; Corresponding PI, 10% (1.2 months); Dr. Koutcher directs the overall project. Funding Support – NIH

Ellen Ackerstaff ~30% - (Co-Investigator) Dr. Ackerstaff supervises all the metabolic studies performed both in vivo and in vitro. Other support – NIH

Avigdor Leftin 50% - 6 months Postdoctoral Fellow – Dr. Leftin performs all the iron MRI imaging and the correlative immunohistochemistry and histology. Other support – NIH. He has gone on to a position of Assistant Professor of Chemistry and Radiology at SUNY Stony Brook. Dr. Ackerstaff has picked up a significant portion of his responsibilities

Natalia Kruchevsky 25%. Works with Dr. Ackerstaff on metabolic studies and Other support NIH. She has left and Mr. Winkleman is being trained to perform her work and Dr. Ackerstaff has also picked up some of her work

Blasberg Laboratory; W81XWH-17-1-0526 (Partnering PI)

Ronald Blasberg: Supporting PI; 10% (1.2 months); Dr. Blasberg directs/supervises many of the cell studies including oxygen consumption measurements, proliferation etc

Taha Merghoub; Co-Investigator (Co-I) 10% (~ 1 month) – supervises flow cytometry and immune studies

Natalia Kruchevsky 25%. Works with Dr. Serganova measurements of tumor cell proliferation, migration, XF-96 measurements of oxygen consumption and glucose utilization. Other support NIH. She has left and Mr. Winkleman is being trained to perform her work

Sadna Budhu – Co-Investigator – 20% - 2.4 calendar months - performs the flow cytometry and immune studies to monitor the effect of DFP on immune cells; Other support - NIH

Inna Serganova – Co-Investigator – 10% (1.2 calendar months); 5% funds – Dr. Serganova is a Senior Research Scientist. She supervises Ms. Kruchevsky for the cell proliferation and migration studies and works with Dr. Budhu. Other support – NIH

Jaya Satagopan Co-Investigator – 0.6 months. Dr. Satagopan is responsible for statistical design and analysis of all experiments. Other support – NIH. She has left, and another statistician is being designated.

Collaborative Award:

This is a collaborative award between Dr. Koutcher and Dr. Blasberg. Note that we have clearly earmarked the contributions of each laboratory

Changes in Other Support:

KOUTCHER, JASON

(NEW)

2 U54 CA137788 11A1 (PI: Ahles/ Koutcher) 9/20/2019 8/31/2024 0.60 calendar NCI

2/2 CCNY MSKCC Partnership for Cancer Research, Education and Community Outreach (Pilot Res Project 002)

This proposal describes our plans to continue and enhance the City College of New York Memorial Sloan Kettering Cancer Center Partnership for Cancer Research, Education and Community Outreach. Role: Principal Investigator

MERGHOUB, TAHA

(NEW)

GC241004 (PI: Wolchok) 9/1/2019 9/1/2021 1.20 calendar
Technology Development Fund $250,000

Targeting IL10R1 to confer sensitivity to immunotherapy across solid cancers

The goal of this project is to use a monoclonal antibody targeting IL10R1 to extend the efficacy of cancer immunotherapy to the approximately 80% of patients with solid cancer that do not benefit from current immunotherapy. We have found that anti IL10R1 enhances the efficacy of agents that stimulate antigen presenting cells, many of which are already FDA approved.

Role: Co PI

ACKERSTAFF, ELLEN

(NEW)

2 U54 CA137788 11A1 (PI: Ahles/ Koutcher) 9/20/2019 8/31/2024 1.20 calendar
NCI

2/2 CCNY MSKCC Partnership for Cancer Research, Education and Community Outreach (Pilot Res Project 002

This proposal describes our plans to continue and enhance the City College of New York Memorial Sloan Kettering Cancer Center Partnership for Cancer Research, Education and Community Outreach.

Role: Co Investigator

Special Reporting Requirements:

Nothing to report.

Memorial Sloan Kettering Cancer Center

Triple-negative Breast Cancer Cell Line 4T1

Paola Porcari[1], H. Carl LeKaye[1], Jason A. Koutcher[1,2,3,4], Ellen Ackerstaff[1]

[1]Department of Medical Physics, [2]Department of Medicine, [3]Molecular Pharmacology Program, Memorial Sloan Kettering Cancer Center, New York, NY, [4]Weill Cornell Medical College, Cornell University, New York, NY

Background

Triple-negative breast cancer (TNBC) ***lacks*** estrogen (ER^-), progesterone (PR^-) and $HER2^-$ receptors, which ***challenge*** the current targeted therapies.

Infiltration of iron-rich tumor-associated macrophages promotes tumor progression.[1,2]

- Cellular iron is essential for cell proliferation[3] and metabolism and ***increases*** cancer cells susceptibility[4] to modest iron deficiency.[5-7]

Deferiprone (DFP), a clinically approved iron chelator for non cancer-related diseases,[8] alters iron-dependent enzyme activities by decreasing cellular iron.[9-11]

- Preliminary data shows the ***cytostatic*** effect of DFP to multiple breast cancer cell lines.

Purpose and Innovation

- To investigate the ***mechanism*** of DFP ***induced cell cytostasis*** and its ***potential*** to improve ***chemotherapeutic treatment response***.
- DFP effectiveness evaluated using live cell multi-nuclear magnetic resonance spectroscopy (MRS).

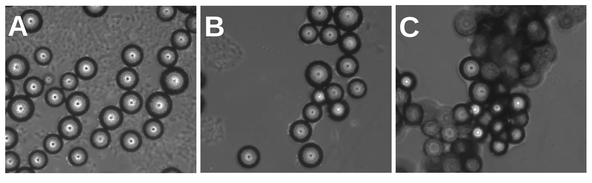

Fig.1 Axial views of cross sectional areas of a Petri dish containing cell seeded on microcarrier beads in DME culture medium. Images A, B and C were acquired on the same Petri dish 24h (A), 48h (B) and 72h (C) following cell seeding.

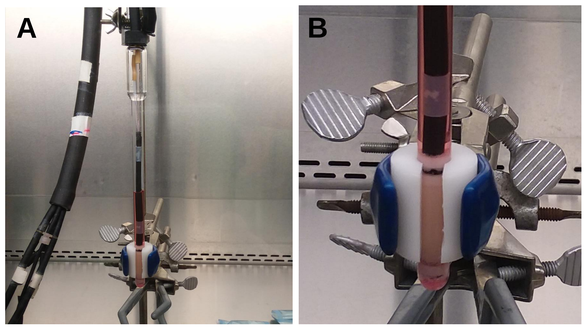

Fig. 2 Perfusion system. **A**, Water jacket connected with the NMR tube where live cells are loaded before the NMR monitoring. The water jacket contains the in-flow and out-flow lines of both medium and carbogen together with those of the circulating warm water. **B**, magnification of the NMR tube showing live cells seeded on microcarrier beads and loaded in the system.

Experimental Design

TNBC model

4T1 murine metastatic cell line.

Bioreactor MR Studies

Cells: 4T1 cells seeded on microcarriers beads [125-212 µm diameter; 3×10^6 cells / 0.5 ml beads × 6]

- Cells grown to near confluence (Fig 1)
- Cell *number* and *viability* estimated at the start and end of each experiment by Trypan Blue exclusion assay

Monitoring Metabolism Changes

- Live, perfused cells in the bioreactor (Fig 2) monitored on a 500 MHz Bruker MR system equipped with a 10-mm broad-band probe
- Cellular energy state measured by 31P MRS (2×30 min spectra every 6h).

  The perfusate exchanged for medium (25mM 1-^{13}C-labeled glucose) 1h after the starting acquisition.
- Metabolization of 1-^{13}C-Glucose measured by ^{1}H decoupled ^{13}C MRS. Spectra (20 min each) continuously acquired for 31 hours (interspaced with ^{31}P spectra).

Quantification: jMRUI software

Metabolites normalized to the β-NTP signal of the first ^{31}P MR spectrum (βNTP_{init}). Data processed as previously reported[5,12].

Three independent experiments performed on DFP-treated (culture medium containing 100 µM DFP) and un-treated cells, respectively.

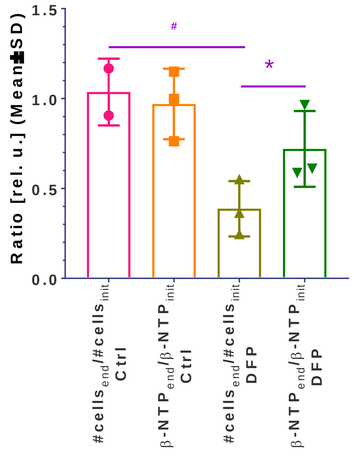

Fig. 3 Comparison between cell growth (ratio of counted cells at the end over counted cells at the start of the experiment ($\#cells_{end}/\#cells_{initial}$]) and the corresponding cellular energy ratio =[$\beta\text{-}NTP_{end}/\beta\text{-}NTP_{init}$] in DFP-treated and 4T1 cells.

Results

- Significantly lower cell mass in DFP-treated than untreated cells shown by the ratio between counted cells at the end and start ($\#cells_{end}/\#cells_{initial}$) of each experiment (Fig 3).
- β-NTP more representative of cell number in control than DFP-treated cells where it decreases significantly slower than the cell loss (Fig 3).
- β-NTP levels, while trending, do not show significant differences between DFP-treated and control 4T1 cells (Fig 4,E).
- Quantitative evaluation of ^{13}C spectra metabolites of DFP-treated cells revealed ***less*** glucose-C1 signal loss, higher glutamine-C4 and fatty acid chains and less Alanine-C3 ^{13}C-labelling than in control (CTRL) cells (Fig 5).

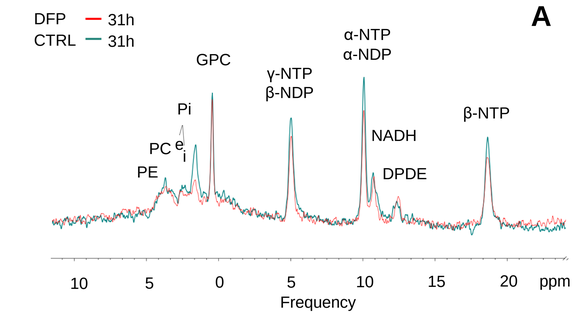

Fig. 4 **A**, Comparison between 31 P spectra of DFP-treated and untreated cells, acquired at the end (B) of the of the experiment (31h). **B**,**C**,**D**: Time course curves for PCho (B), GPCho (C) and β-NTP (D) showing statistical significance ($p < 0.05$, unpaired t-test) between DFP-treated and controls at latest time points (t > 18h). PCho (B) and GPCho (C) changes indicate phospholipid membrane turnover differences between DFP-treated and control cells.
The intracellular pH was stable throughout and unaffected by DFP.

Conclusion

- This study demonstrates that DFP treatment ***affects*** Krebs cycle, energy and fatty acid metabolism.

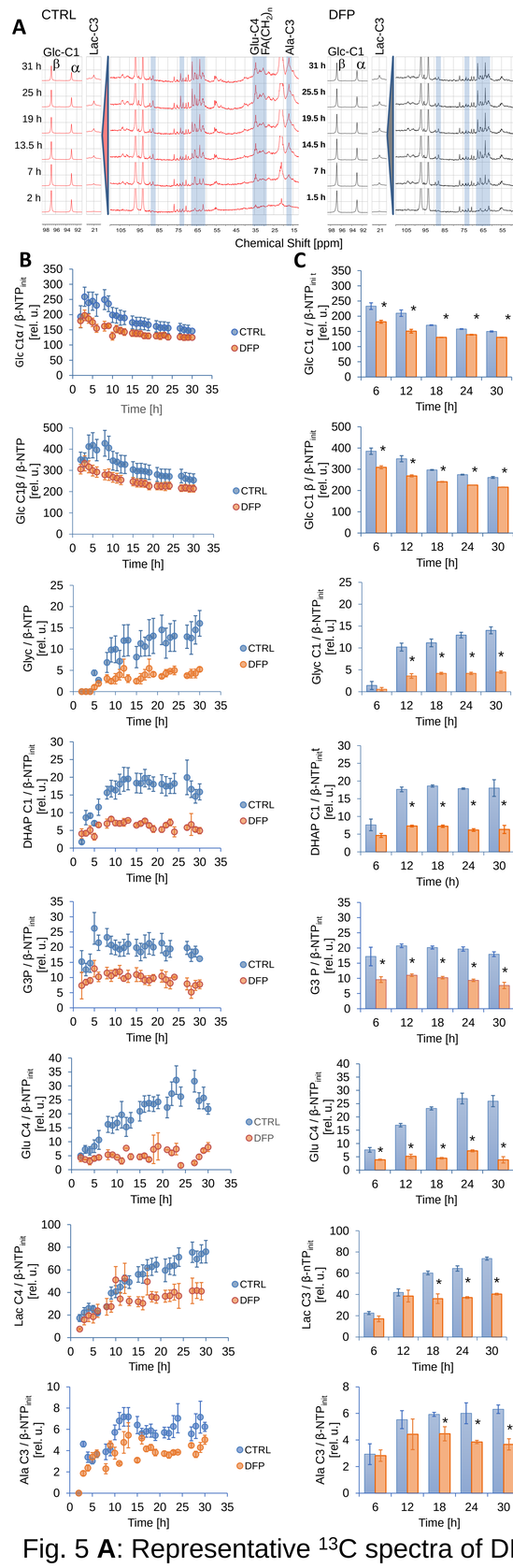

Fig. 5 **A**: Representative ^{13}C spectra of DF treated and untreated cells over time.
B, Time-course effect of DFP on live 4T1 metabolism, as detected by ^{13}C –MRS.
C, Average metabolite synthesis at differ time intervals.
* Significantly different from untreated cell ($p < 0.05$, unpaired Student *t* test)

References

Wang J *et al. Med Sci Monit* 2016 **22**; 2. Yuan ZY *et al. Oncotargets and Therapy* 2014 **7;** 3. Simoes RV *et al.* NMR Biomed 2017 **30**(6); 4. Pinnix ZK *et al Sci Transl Med* 2010 **2**(43); 5. Freitas I *et al. Anticancer Research* 2007 **27**; 6. Hann HW *et al. Cancer Res* 1988 **48**(15); 7. Hann HW *et al. Cancer* 1991 **68**(11); 8. Piga A *et al. Ann N Y Acad Sci* 2010 **1202**; 9. Beinert H *et al. FASEB J* 1993 **7**(15); 10. Glickstein H *et al. Blood* 2005 **106**(9); 11. Goncalves S *et al. BMC Neurol* 2008 **8**; 12. Simoes RV *et al. Neoplasia* 2015 **17**(8)

Acknowledgment

This work was supported by grants W81ZWH-17-1-0525 (JAK) and P30CA008748 (Cancer Center Support Grant)
Thanks to Dr R.V. Simoes for helpful discussion.